Supplementary information, Table S2 Correlation of MPZL1 expression with multiple clinical features of HCC specimens.

Variables		N	MPZL1 expression			χ^2	*p* value
			Upregulation n (%)	Downregulation n (%)	No change n (%)		
Gender	Male	46	19 (41.3)	5 (10.9)	22 (47.8)	0.343	0.842
	Female	12	5 (41.7)	2 (16.6)	5 (41.7)		
Age (Year)	⩽55	40	19 (47.5)	4 (10.0)	17 (42.5)	2.079	0.354
	>55	18	5 (27.8)	3 (16.7)	10 (55.6)		
Edmondson grade	Low	20	5 (25.0)	4 (20.0)	11 (55.0)	4.664	0.097
	High	33	17 (51.5)	2 (6.10)	14 (42.4)		
Intrahepatic metastasis	Present	27	16 (59.3)	1 (3.7)	10 (37.0)	8.95	**0.011(*)**
	Absent	24	5 (20.8)	5 (20.8)	14 (58.3)		
Tumor size (cm)	<5	19	7 (36.8)	1 (5.30)	11 (57.9)	1.948	0.378
	≥5	28	13 (46.4)	4 (14.3)	11 (39.3)		
Serum AFP (ng/ml)	⩽400	29	12 (33.3)	3 (11.1)	14 (55.6)	0.384	0.825
	>400	26	11 (44.7)	4 (13.2)	11 (42.1)		
HBsAg	Present	44	16 (36.4)	7 (15.9)	21 (47.7)	3.39	0.184
	Absent	14	8 (57.1)	0 (0.00)	6 (42.9)		
Cirrhosis	Present	24	8 (33.3)	5 (20.8)	11 (45.8)	3.251	0.197
	Absent	34	16 (47.1)	2 (5.90)	16 (47.1)		

p value represents the probability from χ2 test for MPZL1 expression status between variable subgroups. AFP, alpha-fetoprotein; HBsAg, hepatitis B virus surface antigen. Low grade = 1 or 2; High grade = 3 or 4. *, χ2 test, $p < 0.05$.

Supplementary information, Table S3 Summary of results derived from phospho-antibody array

Phosphorylation sites	HUH-7 VECTOR Ratio	HUH-7 MPZL1 Ratio	Ratio (HUH-7 MPZL1/VECTOR)
MEK1(Phospho-Thr286)	0.34	0.78	2.28
Synapsin(Phospho-Ser9)	0.71	1.17	1.65
PKCalpha/betaII(Phospho-Thr638)	0.87	1.41	1.62
CDC25C(Phospho-Ser216)	0.23	0.36	1.61
FAK(Phospho-Tyr397)	0.59	0.90	1.52
p44/42MAPKinase(Phospho-Thr202)	1.35	1.97	1.46
AKT(Phospho-Ser473)	0.91	1.29	1.42
PLCbeta3(Phospho-Ser537)	0.84	1.19	1.42
PKCalpha(Phospho-Tyr657)	1.30	1.80	1.39
BAD(Phospho-Ser155)	0.92	1.25	1.36
Paxillin(Phospho-Tyr118)	1.65	2.18	1.32
c-Raf(Phospho-Ser296)	0.75	0.99	1.32
SHP-2(Phospho-Tyr580)	0.83	1.09	1.31
Cortactin(Phospho-Tyr421)	1.55	2.01	1.30
CDC25A(Phospho-Ser75)	0.89	1.11	1.25
CDC2(Phospho-Tyr15)	0.98	1.22	1.24
Merlin(Phospho-Ser518)	1.40	1.73	1.24
MKK3/MAP2K3(Phospho-Thr222)	0.79	0.97	1.23
Pyk2(Phospho-Tyr402)	0.82	0.99	1.20
AKT(Phospho-Thr308)	1.34	1.60	1.20
p44/42MAPKinase(Phospho-Tyr204)	1.03	1.23	1.19
Stathmin1(Phospho-Ser15)	0.90	1.07	1.19
Ezrin(Phospho-Tyr353)	0.90	1.06	1.19
Stathmin1(Phospho-Ser24)	0.86	1.01	1.18
Stathmin1(Phospho-Ser37)	0.85	0.99	1.17

BAD(Phospho-Ser112)	1.09	1.28	1.17
Src(Phospho-Tyr416)	0.64	0.74	1.16
MEK1(Phospho-Ser221)	1.08	1.24	1.15
Caveolin-1(Phospho-Tyr14)	0.88	0.99	1.12
SHP-2(Phospho-Tyr542)	1.12	1.23	1.1
VASP(Phospho-Ser157)	0.35	0.39	1.09
GRB2(Phospho-Ser159)	1.14	1.23	1.08
ERK3(Phospho-Ser189)	1.01	1.08	1.06
Connexin43(Phospho-Ser367)	0.91	0.97	1.06
WAVE1(Phospho-Tyr125)	1.03	1.08	1.05
FAK(Phospho-Tyr925)	1.11	1.15	1.04
p130Cas(Phospho-Tyr410)	0.98	1.02	1.04
MEK1(Phospho-Ser298)	0.39	0.40	1.03
CaMKII(Phospho-Thr286)	0.93	0.93	1.00
FAK(Phospho-Tyr407)	0.95	0.95	1.00
cofilin(Phospho-Ser3)	0.87	0.87	0.99
c-Raf(Phospho-Ser43)	0.31	0.31	0.98
CaMK4(Phospho-Thr196/200)	1.05	1.03	0.98
CrkII(Phospho-Tyr221)	2.08	2.02	0.97
ACTINPan(a/b/g)(Phospho-Tyr55/53)	0.67	0.65	0.97
FAK(Phospho-Tyr861)	1.36	1.30	0.96
MKK7/MAP2K7(Phospho-Ser271)	1.04	1.00	0.96
Rho/Racguaninenucleotideexchangefactor2(Phospho -Ser885)	1.23	1.17	0.95
Raf1(Phospho-Ser338)	0.99	0.93	0.94
PLC-beta(Phospho-Ser1105)	0.92	0.86	0.94
Myosinregulatorylightchain2(Phospho-Ser18)	0.88	0.83	0.94
FilaminA(Phospho-Ser2152)	0.99	0.93	0.93
G3BP-1(Phospho-Ser232)	1.29	1.20	0.93

Supplementary information, Table S5 The sequences of siRNAs and shRNA plasmids used

siRNAs/shRNAs	Sequence (5' to 3')	Origin
siRNA-Negative control	TTCTCCGAACGTGTCACGT	Genepharma
siRNA-CTTN-1	GCCACGAAUAUCAGUCGAATT	Genepharma
siRNA-CTTN-2	CAGAAGGUCACGUGGAAAUTT	Genepharma
siRNA-CTTN-3	CACACCUCAUAGGUAUGAUTT	Genepharma
siRNA-Src-1	CAGGCUGAGGAGUGGUAUUTT	Genepharma
siRNA-Src-2	GCCUCAACGUGAAGCACUATT	Genepharma
siRNA-Src-3	CUCGGCUCAUUGAAGACAATT	Genepharma
siRNA-SHP-2-1	GGGCACGAAUAUACAAAUATT	Genepharma
siRNA-SHP-2-2	GAAGCACAGUACCGAUUUATT	Genepharma
siRNA-SHP-2-3	GACCACAGAUAAAGUCAAATT	Genepharma
shRNA-Negative control	ACCTCCACCCTCACTCTGCCAT	Open biosystems,Thermo
shRNA-MPZL1-1	TGACATCACAGATATAGGT	Open biosystems,Thermo
shRNA-MPZL1-2	TCAAGTGGCATAGCCAATG	Open biosystems,Thermo
shRNA-MPZL1-3	CCGAAAGAATTAAGAGAAT	Open biosystems,Thermo

Supplementary information, Table S6 Primers used for q-PCR and subclone

Primers used for q-PCR.

Gene symbol	Forward (5' to 3')	Reverse (5' to 3')	Accession
MPZL1-g/c	CTCCCAAGGGCAAGTGTA	CAACGATGTCAGGAGGGT	NM_003953.5
MPZL1a	AAAACCCTCCTGACATCG	CTAACTGTGCATATATGACTGG	NM_024569.4
MPZL1b	TGGAGTATCAGCCTTGGA	TCCGCATACACCACAGAC	NM_001146191.1
ATP1B1-c	CAGTGAACCGAAAGAACG	ACTGAACGGGAAGGACAT	NM_001677.3
ATP1B1-g	TTGTAGGCGAATCTATGAG	AAGCACTATTTCCCTGACT	NC_000001.10
NEM7-c	TCACCAGTCAAGACCCTT	TCTTATGCCATCTGTTCC	NM_138638.4
NEM7-g	TATGAGCAAGGGCAGTTA	TTGAGTAGGGAAGGAAGG	NC_000014.8
PIGC-c	AGCCCTTTCCTGATAACT	CCAGACCAGTCCCTAAAA	NM_153747.1
PIGC-g	TTCTTCACTGATTGGGTAT	TGACATGGCATAGATGGT	NC_000001.10
LINE-1	AAAGCCGCTCAACTACATGG	TGCTTTGAATGCGTCCCAGAG	NC_000002.11
β-actin	AGTGTGACGTGGACATCCGCAAAG	ATCCACATCTGCTGGAAGGTGGAC	NM_001101.3

g, genomic DNA; c, cDNA. The human MPZL1 consists of 3 isoforms (MPZL1, MPZL1a and MPZL1b) differing in their cytoplasmic sequences.

Primers used for subclone.

Gene symbol	Forward (5' to 3')	Reverse (5' to 3')	Accession
MPZL1-ORF	CGGGATCCATGGCAGCGTCCG	CGGAATTCTTAATTCTTTCGGATATCC	NM_003953.5
CTTN-ORF	CGGGATCCATGTGGAAAGCTTCAGCA	CGGAATTCCTACTGCCGCAGCTCC	NM_005231.3
CTTN-Y421D	CCCCGTCGATGAGGATG	CATCCTCATCGACGGGG	NM_005231.3
CTTN-Y421A	CCCCGTCGCTGAGGATG	CATCCTCAGCGACGGGG	NM_005231.3
CTTN-Y470D	GAGGCTGTCGATGAAAGCG	CGCTTTCATCGACAGCCTC	NM_005231.3
CTTN-Y470A	GAGGCTGTCGCTGAAAGCG	CGCTTTCAGCGACAGCCTC	NM_005231.3
CTTN-Y486D	GACAGCACCGATGATGAGTAC	GTACTCATCATCGGTGCTGTC	NM_005231.3
CTTN-Y486A	GACAGCACCGCTGATGAGTAC	GTACTCATCAGCGGTGCTGTC	NM_005231.3
SRC-ORF	CGACGCGTATGGGTAGCAACAAGAGC	CGGAATTCCTAGAGGTTCTCCCCGG	NM_005417.3
SRC-K298M	TGGCCATCATGACCCTGA	TCAGGGTCATGATGGCCA	NM_005417.3
	ACCTGCAGGCCTTCCTGGAGGACTAC	CGGAATTCCTAGAGGTTCTCCCCGGGCTG	
SRC-Y530F	TTCACGTCCACCGAGCCCCAGTTCCA	GAACTGGGGCTCGGTGGACGTGAAGTAG	NM_005417.3
	GCCCGGGGAGAACCTCTAG	TCCTCCAGGAAGGCCTGCAGGT	

*, the isoform a (full length MPZL1) of MPZL1 was used in this study (Accession number: NM_003953.5).

Supplementary information, Table S7 Clinical and pathological features of 58 HCC specimens

ID	Gender	Age (y)	HBsAg	anti-HCV	Cirrhosis	Edmondson grade	Intrahepatic metastasis	Serum AFP level (ng/mL)
HK08	M	52	+	-	Y	III	-	2347.5
HK14	M	55	+	+	N	IV	-	11224.3
HK17	M	47	+	-	Y	III	-	495.4
HK26	M	42	+	-	Y	III	+	632.8
HK31	M	66	+	-	Y	I	+	11.4
HK32	F	60	+	-	Y	I	-	6.2
HK35	M	55	+	-	Y	I	-	2769.7
HK38	M	58	+	-	Y	II	-	104.9
HK39	M	57	-	-	N	II	+	84.7
HK41	M	46	-	-	N	III	+	2.8
HK42	M	58	+	-	Y	I	-	871.3
HK43	M	62	+	-	Y	I	-	12.9
HK51	M	42	+	-	Y	III	+	Null
HK54	M	31	+	-	N	II	+	576.6
HK56	M	50	+	-	N	III	+	110.6
HK60	M	52	-	-	N	II	-	158526
HK70	M	43	+	-	N	IV	+	7572.4
HK71	M	59	+	-	Y	II	-	621
HK80	M	75	+	-	Y	Null	Null	10.7
QD127	M	43	+	-	N	IV	+	Null
QD128	M	42	+	-	Y	III	+	<20
QD130	F	45	+	Null	Y	Null	Null	>400
QD131	M	41	+	Null	N	Null	Null	<20
QD132	M	56	-	Null	N	II	-	380
QD133	M	66	+	-	Y	III	+	328
QD134	M	45	+	-	N	III	-	>400
QD135	F	44	-	-	N	IV	+	<20
QD136	M	34	-	+	N	IV	+	<20
QD137	M	52	-	+	N	II	-	<20
QD138	M	60	+	-	N	IV	+	200
QD152	M	45	+	-	Y	III	+	320
QD153	M	47	+	-	N	IV	-	>400
QD154	M	48	+	-	N	II	-	>400
QD155	F	66	+	-	N	III	+	>400
QD156	M	42	+	-	N	III	-	40
QD157	F	51	+	-	N	II	-	300
QD161	M	48	+	-	N	II	Null	>400
QD162	F	67	+	+	N	III	-	250
QD166	F	54	-	-	N	III	+	>400

QD313	F	46	+	Null	Y	II	+	859
QD314	M	63	+	-	N	II	-	10
QD315	M	44	+	-	Y	III	+	362
QD316	M	50	+	-	N	III	+	6
QD317	M	47	+	Null	N	IV	+	8
QD318	F	49	+	Null	Y	III	+	766
QD321	M	66	+	-	Y	III	-	>1000
QD323	M	46	+	Null	Y	II	-	517
QD336	M	32	+	Null	N	III	+	735
QD337	M	36	+	Null	Y	III	+	701
QD338	M	49	-	Null	N	IV	+	11.7
QD339	F	54	+	-	N	III	-	624
QD340	M	74	-	Null	N	III	-	Null
QD341	F	43	-	Null	N	IV	+	464
QD343	M	69	+	Null	N	IV	-	303
QD344	M	72	+	Null	Y	II	-	415
QD345	M	50	+	Null	Y	III	+	9
QD346	M	61	-	Null	N	IV	-	261.6
QD347	M	52	+	Null	N	II	+	728

Notes: HBsAg, hepatitis B surface antigen; anti-HCV, antibody against HCV, Null, not available. Gender ratio M/F is 47/11, the age ranges from 31-75, with HBV infection positive/negative 46/12 and HCV infection positive/negative 4/37 as well as 17 Null. Hepatocirrhosis positive/negative is 24/34, and intrahepatic metastasis positive/negative is 28/26 as well as 4 Null. Serum AFP level over 400 ng/mL is 27 cases (46.6%).

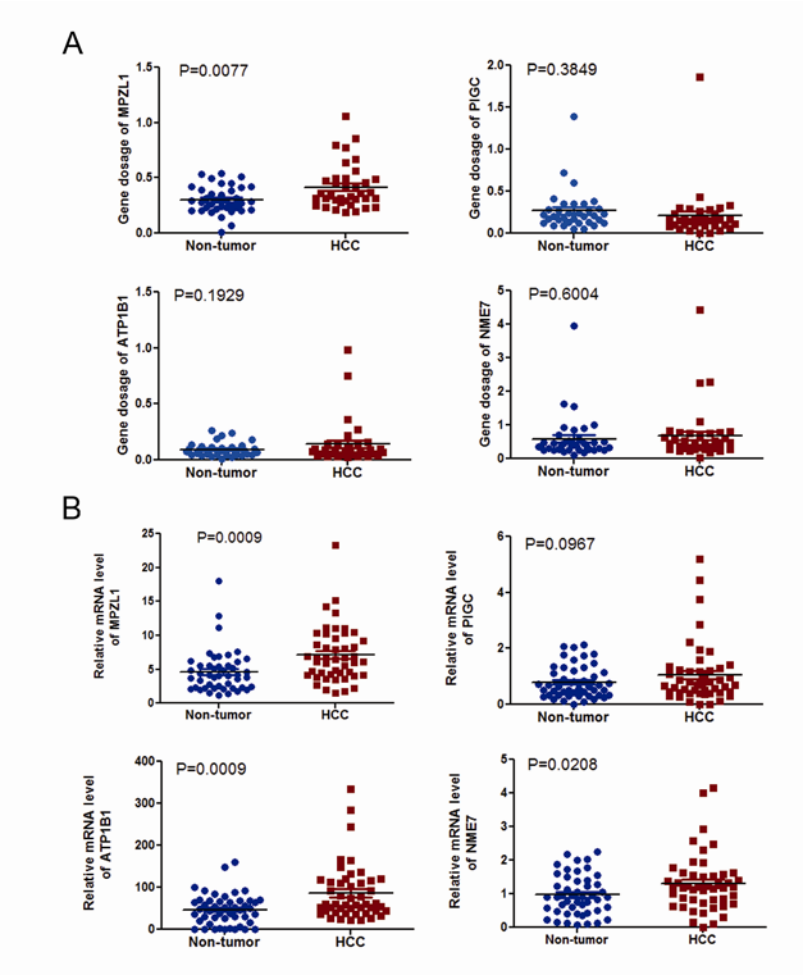

Supplementary information, Figure S1 Examination of the DNA dosages and expression levels of four candidate genes in HCCs. **(A)** Validation of DNA dosages of four candidate genes (*MPZL1*, *ATP1B1*, *NME7* and *PIGC*) by q-PCR in 37 paired HCCs. **(B)** Validation of gene expression of four candidate genes by q-PCR in 49 paired HCCs. Statistical analysis of differences between groups was performed by paired Student's *t* test. Results are shown as the mean ± s.e.m and $P < 0.05$ was considered statistically significant.

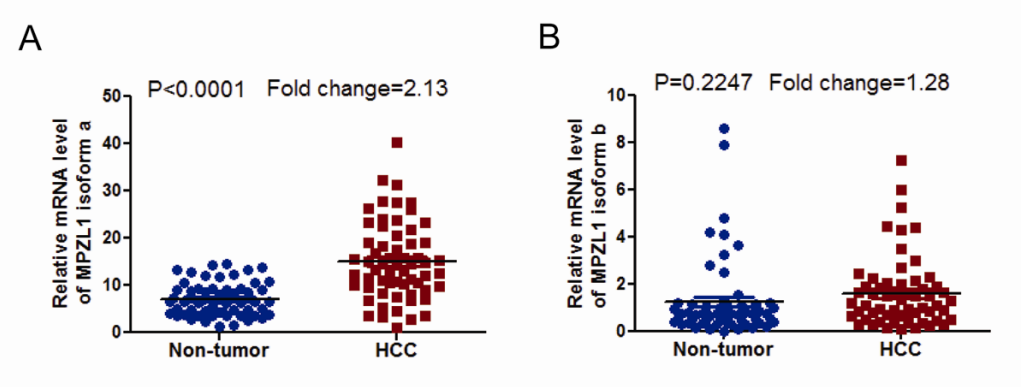

Supplementary information, Figure S2 Examination of the relative expression levels of MPZL1 isoforms in HCCs. q-PCR analysis of the relative expression levels of isoform a **(A)** and isoform b **(B)** in 58 paired HCCs. Statistical analysis of differences between the two groups was performed by paired Student's *t* test and $P < 0.05$ was considered statistically significant.

There are three isoforms of MPZL1 [1-3]. The variant 1 represents the longest transcript, with a coding region of 810 bp, and encodes the longest isoform a, also known as MPZL1. The variant 2 lacks an alternate coding exon compared to variant 1, which causes a frameshift, with a coding region of 630 bp. The resulting isoform b is shorter and has a distinct C-terminus compared to isoform a, also known as MPZL1a. The variant 3 lacks three alternate exons in the 3' coding region that results in a frameshift, compared to variant 1, with a coding region of 360 bp. The encoded isoform c is shorter than isoform a, also designated as MPZL1b.

The three isoforms are all type 1 transmembrane glycoproteins with identical extracellular and transmembrane domains, but differ in their cytoplasmic tails. The MPZL1 intracellular domain contains two SHP-2 binding immunoreceptor tyrosine-based inhibitory motifs (VIY^{246}AQL and VVY^{263}ADI) which are not present

in MPZL1a and MPZL1b, whereas the MPZL1a and MPZL1b isoforms could directly interact with MPZL1 and inhibit the ability of MPZL1 to interact with SHP-2. Recently, it has been demonstrated that the MPZL1, but not the MPZL1a and MPZLb, may be involved in regulation of integrin-mediated cell motility. However, overexpression of MPZL1a in human HT-1080 cells had a dominant negative effect by blocking concanavalin A (ConA)-induced tyrosine phosphorylation of full-length MPZL1 and recruitment of tyrosine phosphatase SHP-2. Therefore, MPZL1a may have an important role in cell signaling by counteracting with MPZL1. In this study, the isoform a (full-length MPZL1) was employed to determine the functional roles of MPZL1 in HCC. Furthermore, we also examined the relative expression levels of three isoforms of MPZL1 in 58 pairs of HCC and adjacent non-tumor tissues by quantitative real-time PCR (q-PCR). We found that only the isoform a (MPZL1) are overexpressed in HCC compared with adjacent non-tumor tissues, and positively correlated with the intrahepatic metastasis of HCC (Figure 2 and Supplementary Table S2). However, there is no significant difference between HCC and paired adjacent non-tumor tissues for the expression level of MPZL1a (Supplementary Figure S2). Additionally, we could not amplify the sequence and detect the expression status of isoform c (MPZL1b) in HCC and adjacent non-tumor tissues by q-PCR assays.

References:

1. *The Journal of biological chemistry* 1998; **273**:29367-29372;
2. *Biochem J* 2003; **370**:537-549.
3. *Biochemical and biophysical research communications* 2003; **303**:1028-1033.

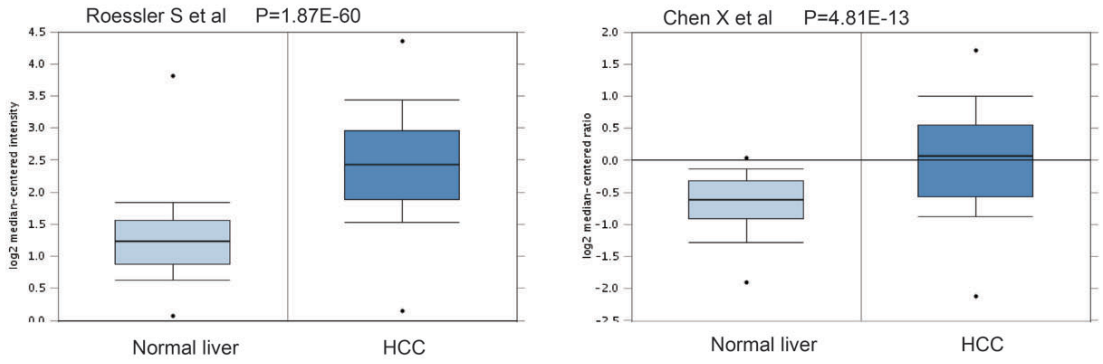

Supplementary information, Figure S3 The expression levels of MPZL1 in HCC derived from gene expression arrays. Boxed plot of MPZL1 expression levels in HCC cancer patients using Oncomine expression analysis [1].

Reference:

1. *Neoplasia* 2004; 6:1-6

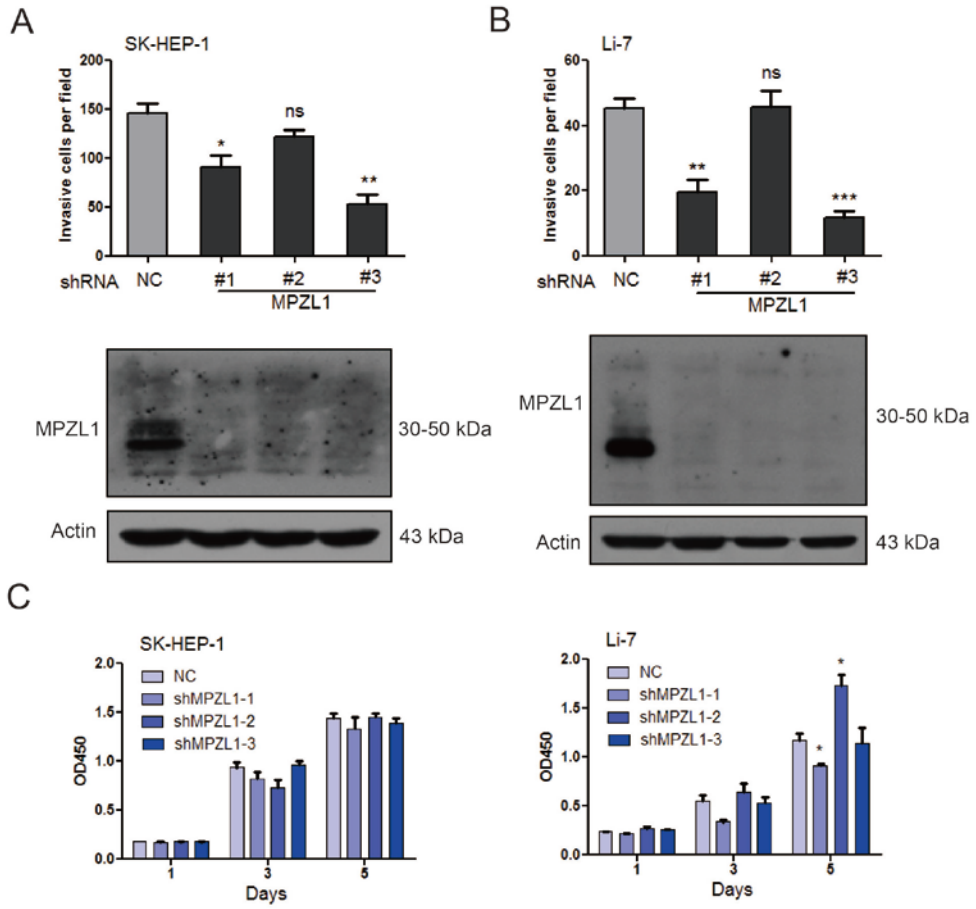

Supplementary information, Figure S4 Knockdown of the *MPZL1* gene inhibited HCC cell migration, but not cell proliferation. (**A, B)** The effects of the MPZL1 gene on the invasive abilities of SK-HEP-1 and Li-7 cells by Trans-well migration assays. All the results are shown as the mean ± s.e.m. **P* < 0.05; ***P* < 0.01; ****P* < 0.001. The detection of the shRNA-mediated knockdown of the *MPZL1* gene in SK-HEP-1 and Li-7 cells by immunoblotting. **(C)** Representative result of CCK-8 assays for the effects of *MPZL1* gene on the *in vitro* proliferation of SK-HEP-1 and Li-7 cells by lentivirus-mediated knockdown. The results are shown as the mean ± s.e.m. **P* < 0.05.

In the current study, we have employed three shRNAs to knockdown the *MPZL1* gene.

The knockdown efficiency of each shRNA was examined by immnuoblotting. The results showed that all of the three shRNAs can significantly knockdown the *MPZL1* gene. However, only two shRNAs (shMPZL1-1 and shMPZL1-3) can effectively inhibit the migratory ability of HCC cells. Moreover, we found that the shRNA-MPZL1-3 was the most effective in suppressing cell invasion. In addition, knockdown of *MPZL1* gene by the shRNA-MPZL1-3 has no significant effect on HCC cell proliferation. Therefore, the shRNA-MPZL1-3 was further used in the next study.

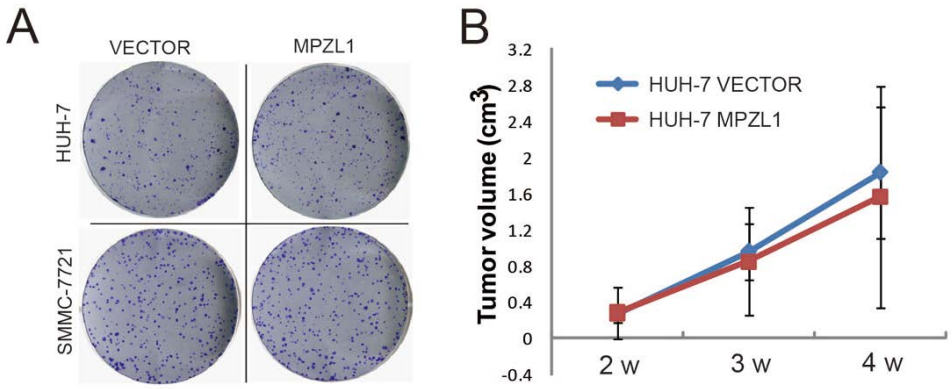

Supplementary information, Figure S5 Enforced expression of *MPZL1* has no significant effect on HCC cell proliferation. **(A)** Representative result of colony formation assays for the effects of *MPZL1* overexpression on the *in vitro* proliferation of Huh-7 and SMMC-7721 cells. **(B)** The effects of *MPZL1* on the *in vivo* growth abilities of HUH-7 cells in xenograft mouse models by subcutaneously (s.c.) inject tumor cells into the right upper flank region of the nude mice (n=7). Statistical analysis of differences between groups was performed by unpaired Student's *t* test. Results are shown as the mean ± s.e.m and $P < 0.05$ was considered statistically significant.

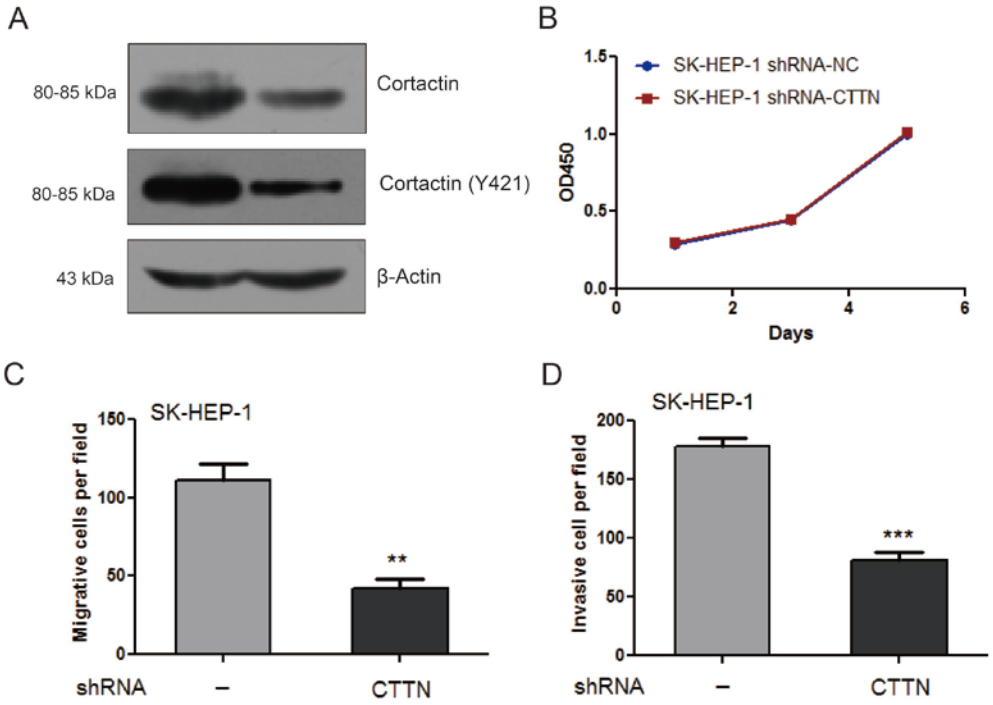

Supplementary information, Figure S6 Knockdown of the *CTTN* gene inhibits the migratory and invasive abilities of HCC cells. **(A)** The detection of the shRNA-mediated knockdown of the *CTTN* gene in SK-HEP-1 cells by immunoblotting. **(B)** A representative result of the CCK-8 assays for the effects of *CTTN* knockdown on the *in vitro* proliferation of SK-HEP-1 cells. **(C, D)** Representative results of the trans-well assays for the effects of *CTTN* knockdown on the *in vitro* migratory and invasive abilities of SK-HEP-1 cells (unpaired Student's t test, the mean ± s.e.m, $^{**}P < 0.01$; $^{***}P < 0.001$).

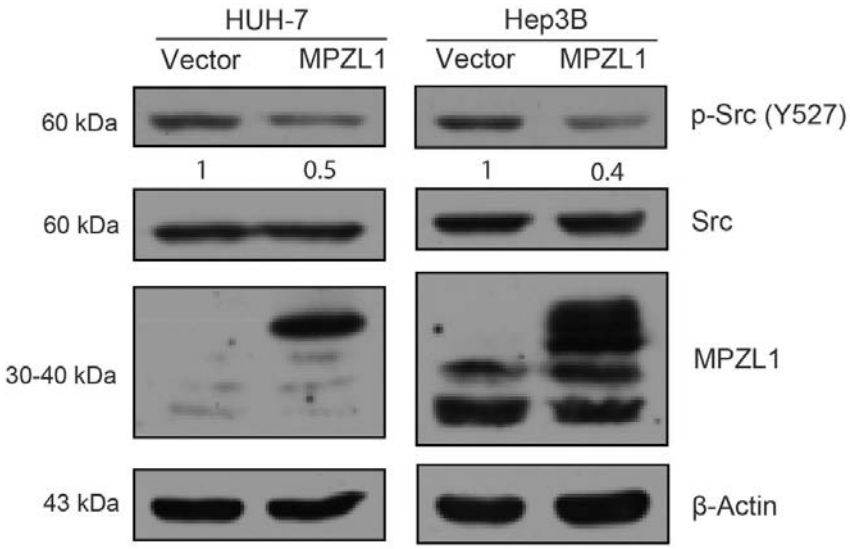

Supplementary information, Figure S7 Ectopic expression of *MPZL1* leads to decreased phosphorylation levels of negative regulatory site of Src (Y527). The overexpression of *MPZL1* in HUH-7 and Hep3B cells decreases the phosphorylation of Src (Y527) protein.

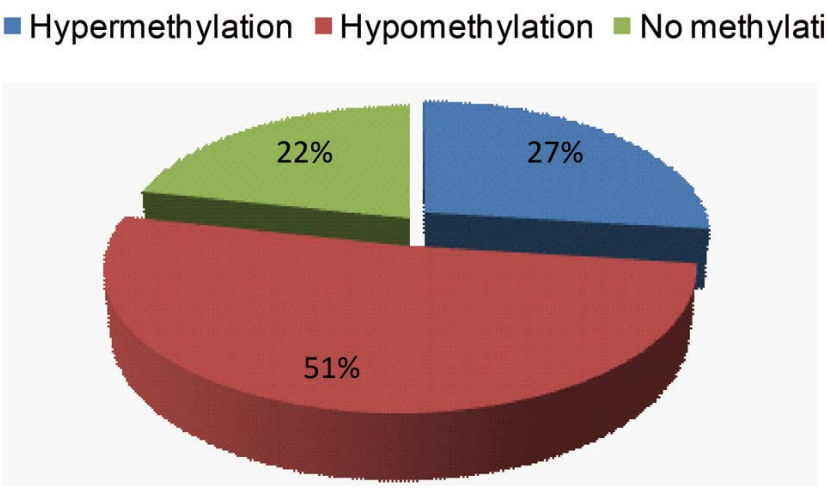

Supplementary information, Figure S8 The Detection and quantitation of *MPZL1* methylation in 37 paired HCC and adjacent paracancer tissues by real-time methylation-specific PCR. We examined the methylation status of CpG islands within *MPZL1* promoter using quantitative real-time methylation-specific PCR on 37 cases of paired HCC and non-tumor tissues. Totally, 35 out of 37 HCC tissues were methylation-positive. Furthermore, among the 35 methylation-positive HCC cases, the methylation of *MPZL1* promoter was also observed in 33 corresponding non-tumor tissues. However, the methylation levels in 17 HCC tissues were lower than those in the corresponding non-tumor tissues. In summary, the frequency of hypomethylation was approximately 51.4% (19/37) in HCCs, which accounted for the upregulation of *MPZL1* mRNA level in HCC tissues in addition to that caused by genomic gain of 1q24.1-24.2 loci.

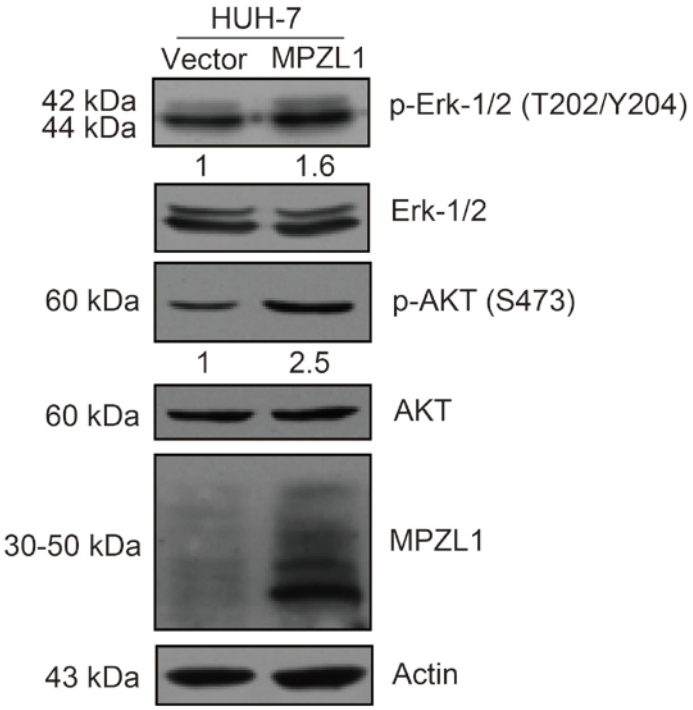

Supplementary information, Figure S9 The overexpression of *MPZL1* in HUH-7 cells induces the phosphorylation of the Erk-1/2 (T202/Y204) and AKT (S473) proteins.

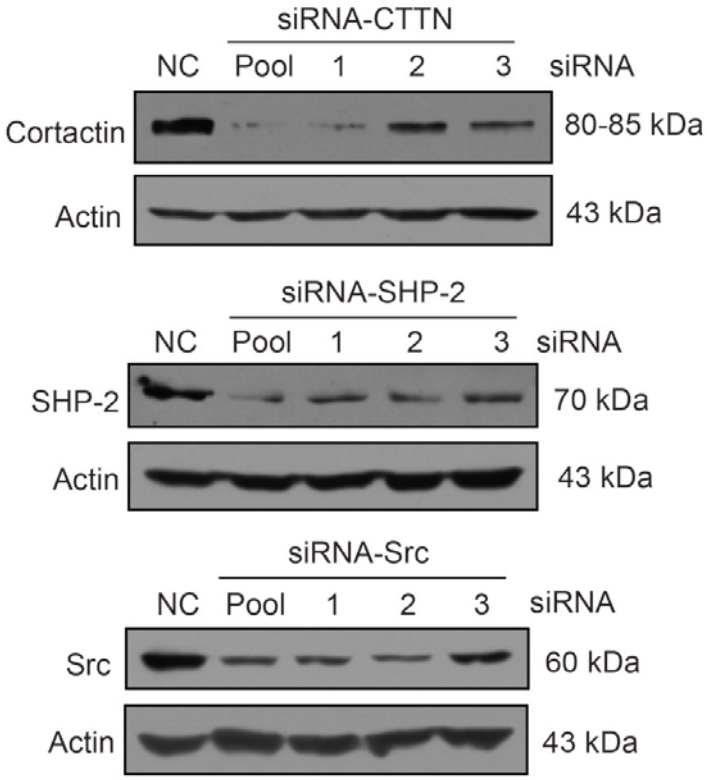

Supplementary information, Figure S10 The detection of siRNA mediated knockdown of targeted genes (*CTTN*, *SHP-2* and *Src*) in HCC cells by immunoblotting. In the current study, three different siRNAs were used to target the *CTTN*, *Src* and *SHP2* gene, respectively. The knockdown efficiency of each siRNA was examined by immnuoblotting. Recently, siRNA pool has been widely used in RNA interference assays [1, 2]. For the Src and SHP-2 genes, we employed siRNA pools (mixture of three different siRNAs) against individual genes, and the results showed that the siRNA pool and each siRNA can significantly knockdown the target genes. For the *CTTN* gene, all the three siRNAs can significantly knockdown this

gene. Subsequently, the siRNA sequence that was most effective in targeting *CTTN* (siRNA-CTTN-1) was used further to construct shRNA vectors.

References:

1. *Nature* 2004; 427:541-544.

2. *Nat Rev Genet* 2006; 7:373-384